Tuning spin-orbit coupling and superconductivity at the $SrTiO_3/LaAlO_3$ interface: a magneto-transport study

M. Ben Shalom, M. Sachs, D. Rakhmilevitch, A. Palevski, and Y. Dagan[1,*]

[1] *Raymond and Beverly Sackler School of Physics and Astronomy, Tel-Aviv University, Tel Aviv, 69978, Israel*

(Dated: January 7, 2010)

The superconducting transition temperature, T_c, of the $SrTiO_3/LaAlO_3$ interface was varied by the electric field effect. The anisotropy of the upper critical field and the normal state magneto-transport were studied as a function of gate voltage. The spin-orbit coupling energy ϵ_{SO} is extracted. This tunable energy scale is used to explain the strong gate dependence of the mobility and of the anomalous Hall signal observed. ϵ_{SO} follows T_c for the electric field range under study.

PACS numbers: 75.70.Cn, 73.40.-c

Interfaces between strongly correlated oxides exhibit a variety of physical phenomena and are currently at the focus of intensive scientific research. An electronic reconstruction occurring at the interfaces may be at the origin of these phenomena.[1] It has been demonstrated that the interface between $SrTiO_3$ (STO) and $LaAlO_3$ (LAO) is highly conducting, having the properties of a two dimensional electron (2DEG) gas. [2] At low temperatures the 2DEG has a superconducting ground state, whose critical temperature can be modified by an electric field effect.[3] The origin of the charge carriers and the thickness of the conducting layers are still under debate. [1, 4–9] Recently, we have demonstrated that for carrier concentrations at the range of 10^{13} cm^{-2}, a large, highly anisotropic magnetoresistance (MR) is observed.[10] Its strong anisotropy suggests that it stems from a strong magnetic scattering confined to the interface.

Here we show that both superconducting and spin-orbit (SO) interaction can be modified by applying a gate voltage. The upper critical field applied parallel to the interface, $H_{c2\|}$, is approximately the weak coupling Clogston-Chandrasekhar paramagnetic limit: $\mu_0 H_{c2} \cong 1.75 k_B T_c$ for high carrier concentrations. However, as the density of the charge carrier is reduced, $H_{c2\|}$ becomes as large as five times this limit, suggesting a rapidly increasing SO coupling. This SO coupling energy ϵ_{SO} manifests itself in many of the transport properties studied.

We use a sample with 15 unit cells of $LaAlO_3$, deposited by pulsed laser on an atomically flat $SrTiO_3(100)$ substrate. The oxygen pressure during the deposition was maintained at 10^{-4} Torr. The deposition was followed by a two-hour annealing stage at oxygen pressure of 0.2 Torr and a temperature of 400 C. The thickness of the $LaAlO_3$ layer was monitored by reflection high energy electron diffraction. Growth procedure is similar to the one described elsewhere.[10] A layer of gold was evaporated at the bottom of the sample and used as a gate when biased to ±50 V relative to the 2DEG. Contacts were made using a wire bonder in a Van Der Pauw geometry. We took extra care to ensure the absence of heating by testing the resistance to be current-independent

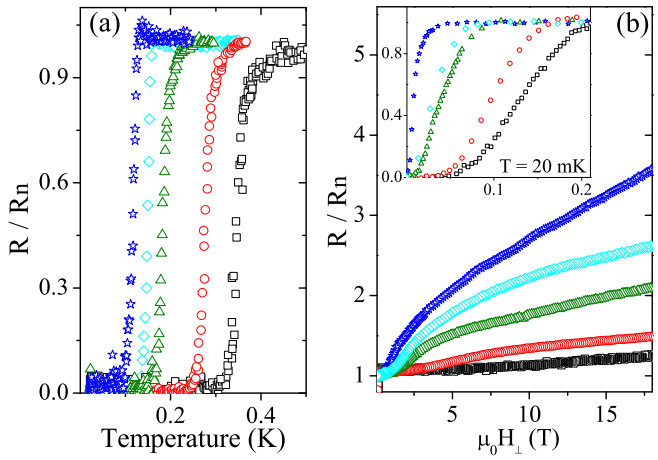

FIG. 1: Color on-line (a) Normalized sheet resistance *versus* temperature for the various gate voltages (from left to right) V_g=50 V, as-grown state, 10 V, -10 V, -50 V color and shape code applies to all graphs in the paper. (b) Resistivity *versus* the perpendicular magnetic field . Inset: zoom on the low field region where superconductivity is suppressed.

at the superconducting transition point, where current sensitivity is maximal. During measurements, the sample was cooled down to a base temperature of 20 mK and a magnetic field of up to 18 T was applied. Samples rotation was done using a step motor with a resolution of 0.015°/step. All transport properties reported here were measured in the as-grown state (AG), and while applying V_g=50, 10, -10, -50 V. In order to accurately determine T_c, the remnant magnetic field was minimized by oscillating the field down to zero. In addition, the sample was kept parallel to the field where superconductivity is less sensitive to it.

Fig.1a presents the normalized resistance R/R_n as a function of temperature for the various V_g values. R_n is the resistance measured at zero field and at T=0.5 K, well above T_c, for each V_g. Tuning V_g from +50 to -50 V increases T_c from 0.1 to 0.35 K.

Fig.1b presents the resistance normalized with R_n *versus* the perpendicular magnetic field at T=20 mK.

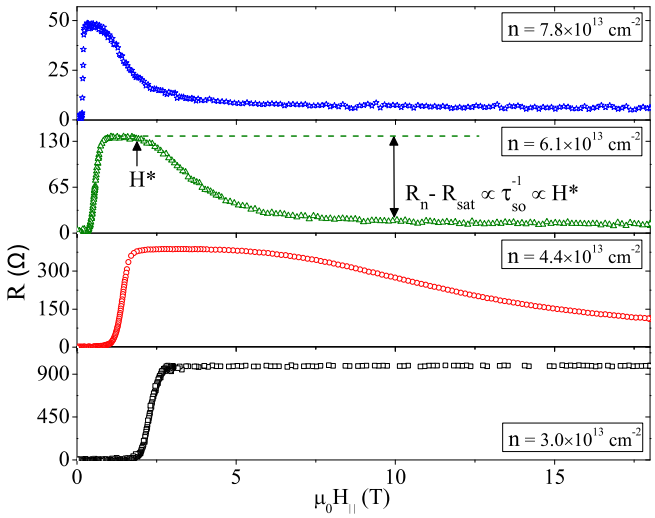

FIG. 2: Sheet resistance *versus* the magnetic field applied parallel to the interface and current for various charge densities.

A large, positive MR is observed for V_g=50 V. Its magnitude gradually decreases as V_g is reduced. The inset zooms on the superconducting low field region.

Table 1 summarizes the superconducting properties for the various V_g. We define $H_{c2\perp}$ (T_c) as the field (temperature) at which the resistance is $R_n/2$. The Ginzburg Landau coherence length $\xi_{GL} = \sqrt{\Phi_0/2\pi\mu_0 H_{c\perp}}$ is extracted from $H_{c2\perp}$, here Φ_0 is the flux quantum.

The charge carrier density $n = 1/R_H e$ is inferred from Hall measurements in the high field regime ($\mu_0 H$ >14 T). It is presented together with the calculated mobility $\mu = n/R_n$. A large variation of μ is observed, indicating a significant change in the scattering rate with gate voltage as previously noted.[11] This behavior will be discussed later.

Fig.2 presents the sheet resistance *versus* the magnetic field, $H_\parallel$, applied parallel to the interface and to the current. From the low field regime we extract the superconducting parallel critical field $H_{c2\parallel}$=H(R_n/2). We note that while T_c increases merely to 0.35 K, $H_{c2\parallel}$ becomes as large as 2.5 T [table 1]. The high $H_{c2\parallel}$ and low T_c implies that the paramagnetic limit is exceeded.[12] Since ξ_{GL} is rather large, 50-200 nm, it is reasonable to use the weak coupling BCS approximation. Accordingly, we expect superconductivity to exist in fields lower than $g\mu_B H \leq 3.5 k_B T_c$; here g is the gyromagnetic ratio and μ_B is the Bohr magneton.

In Fig.3a $\mu_B H_{c2\parallel}$ is plotted against $k_B T_c$ for different V_g values. The dashed straight line represents the paramagnetic limit using BCS weak coupling and g=2. As T_c increases, the limit is exceeded by up to a factor of $\sim$ 5. This behavior suggests a strong SO coupling that relaxes the Clogston-Chandrasekhar limitations.[12] For a superconducting layer thickness $d \ll \xi_{GL}$ it is expected that $H_{c2\parallel}$ be much larger than $H_{c2\perp}$. In this case the critical field is determined by the paramagnetic limit and the spin-orbit energy. From Fig.3a it appears that even for the lowest T_c, superconductivity is quenched in this paramagnetic limit. We can therefore merely set an upper limit on the thickness of the conducting layer by analyzing the anisotropy of the critical field: $d \leq \sqrt{3}\Phi_0/\pi\xi_{GL}\mu_0 H_{c2\parallel}$. [13] The thickness upper limit is presented for the various V_g reaching a minimal value of 10 nm for $n = 3\times10^{13} cm^{-2}$ [table 1]. Previous estimations obtained similar values. They, however, relate d to the actual thickness.[14, 15]

Let us describe the general behavior of R($H_\parallel$) [Fig.2] using the $n = 6.1\times10^{13} cm^{-2}$ curve (green triangle) as an example: Above the superconducting transition, the sheet resistance reaches a roughly field-independent regime (0.9-1.8 T) in which the resistance approximately equals R_n. We define H^* as the onset field where dR/dH becomes negative. For H>H^* the resistance drops to R_{sat}, the low resistance saturation regime ($H_\parallel$>10 T). Both $H_{c2\parallel}$ and H^* strongly depend on V_g; they increase as V_g changes from 50 to -50 V, and H^* becomes unmeasurably high for V_g=-50 V (black squares).

TABLE I:

Vg	n×10^{13}	Mobility	Tc	$\mu_0 Hc_\perp$	$\mu_0 Hc_\parallel$	d	ξ_{GL}	ϵ_{SO}
V	cm^{-2}	cm/secV	K	T	T	nm	nm	meV
-50	3.0	236	0.35	0.125	2.23	10	51	>2
-10	4.4	392	0.28	0.098	1.37	14.4	58	0.58
10	6.1	762	0.18	0.040	0.52	24.1	90	0.21
50	7.8	1707	0.12	0.009	0.14	41.2	194	0.06
AG	9.5	897	0.15	0.030	0.25	44	103	0.12

Fig.3a suggests that SO coupling plays a major role in the system. We shall now describe the data presented so far using a single energy scale, ϵ_{SO}. We relate H^* to the breakdown field of the spin-orbit coupling energy: $g\mu_B H^* = \epsilon_{SO}$. The ϵ_{SO} values are presented assuming g=2 [table 1]. Above this field SO scattering is suppressed and completely vanishes at the high field saturation regime where all spins are aligned. In this scenario the high field saturation value R_{sat} is the remnant impurity scattering. The SO scattering rate can be evaluated from the difference between R_n and R_{sat}. Therefore R_n-R_{sat} should be proportional to $h/\tau_{SO} = \epsilon_{SO}$.

Fig.3b presents $R_n - R_{sat}$ and $\mu_B H^*$ *versus* $k_B T_c$. These two quantities scale as predicted. Furthermore, the saturation resistance R_{sat} roughly scales with the number of carriers. We further use the calculation of R. A. Klemm *et al.* which estimates the SO scattering time from $H_{c2\parallel}$ and T_c for a two-dimensional film in the paramagnetic limit.[16] As seen [Fig.3b, red circles], the general behavior is described by this (probably oversimplified) model. We can therefore conclude that a single energy scale, tuned by V_g, dominates the behavior of the

transport and affects superconductivity. For the carrier concentration range under study $R_{sat} \ll R_n$. Hence, the main contribution to the zero field resistance comes from SO scattering. This explains the strong dependence of the mobility on gate voltage.

We note that for $V_g = 50$ V the carrier concentration is lower compared to the as-grown state. This is in contrast to a simple capacitor-like behavior with negative charge carriers. Furthermore, despite the decrease in carrier concentration, R_n unexpectedly decreases. We relate this peculiar behavior to the SO scattering processes dominating R_n. We assume that static positive charges move to the interface when the highest positive voltage is applied and consequently n is reduced. This charge movement reduces the initial electric field at the interface and as a result decreases the SO scattering. Upon reducing the gate voltage from its maximal positive value, electrons are drawn away from the interface in a reversible manner as expected, and an electric field is created. The initial electric field in the as-grown state results in enhanced SO scattering and higher resistance, despite the higher carrier concentration.

The MR presented [Fig.1b, Fig.2] is highly anisotropic for high magnetic fields. For example, for $n = 6.1 \times 10^{13} cm^{-2}$ and H=18 T, the resistance vary from $0.12R_n$ to $3.5R_n$ (a factor of 30) for the in-plane and out-of-plane field configurations respectively. We study this anisotropy by rotating the sample around an in-plane axis which is perpendicular to the current, while keeping the total field constant, $|\vec{H}|$ =18 T. Fig.4a presents the normalized sheet resistance *versus* the perpendicular field component. For the small angle range presented, the parallel field component is approximately constant $\simeq$18 T. Moreover, for this parallel field component, the resistance is insensitive to small changes in $H_{\|}$[Fig.2]. As shown, the sheet resistance rapidly increases when a small perpendicular component is introduced. It reaches R_n for $H_{\perp} \simeq 1.5$ T (an angle of about 4°). This is similar to our previous observation at 2 K.[10] The curves $n = 7.8, 6.1 \times 10^{13} cm^{-2}$ and AG (not shown) merge near 1.5 T, while $n = 4.4 \times 10^{13} cm^{-2}$ departs form the general behavior. This can be easily explained since for this gate voltage the resistance does not saturate up to 18 T [Fig.2]. For $n = 3.0 \times 10^{13} cm^{-2}$, H=18 T is well below H^* and therefore the anisotropy cannot be observed at this too small a magnetic field. We relate the sudden appearance of resistance with a small perpendicular field component to the orbital motion generated by this component. This motion is enhanced by the high mobility state ($R \simeq R_{sat}$) induced by the presence of a large parallel magnetic field.

Fig.4b presents the Hall resistivity ρ_{xy} at 20 mK *versus* the magnetic field after subtracting out the linear term obtained from a fit to the high field regime. A conspicuous deviation from this linear part in the Hall resistivity (anomalous Hall effect AHE), is observed. This

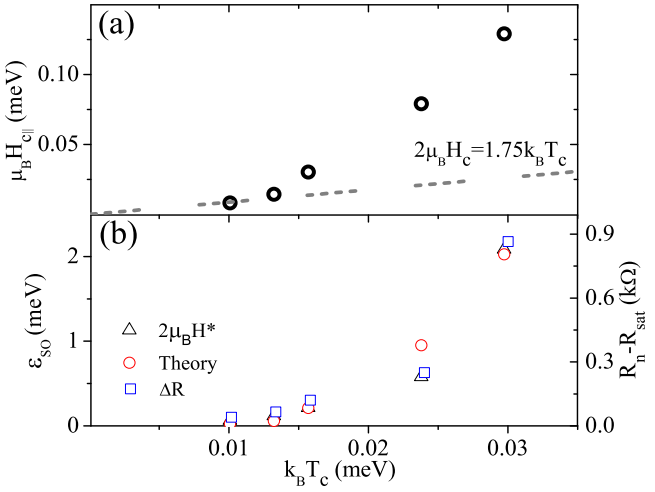

FIG. 3: (Color on-line) a. The parallel upper critical field $H_{c\|}$ *versus* $k_B T_c$ while V_g is varied. The dashed line represents the expected behavior for the paramagnetic limit.
b. ϵ_{SO} extracted from H^* [see Fig.2], and calculated from the measured superconducting properties ($H_{c2\|}$ and T_c),[**?**] *versus* $k_B T_c$. The right axes presents ΔR, which scales with ϵ_{SO} as expected.

AHE persists up to 100 K with a peculiar, roughly linear temperature dependence (not shown). As shown, the applied V_g varies the AHE saturation field. This variation is inconsistent with a simple magnetic impurity scenario and with a simple ferromagnetic behavior. Furthermore, no hysteresis is observed for all carrier concentrations. Here we note that the AHE saturation field roughly follows the behavior of ϵ_{SO} and may be related to it.

Fig.4c compares the data in Fig.4b in the case where $n = 4.4 \times 10^{13} cm^{-2}$ (red circles), with data taken at constant magnetic field while rotating the sample (as in Fig.4a). For the rotation (brown pluses), the slope of the AHE is much steeper. The two measurements differ at low perpendicular fields where the mobility is an order of magnitude higher for the rotation. The qualitative variation between the measurements is expected since the AHE is usually proportional to some power of the resistivity. The AHE has been related to a multiple band structure (light and heavy)[11] and to incipient disordered magnetism induced by the field[17]. The former is unlikely in view of the strong AHE slope in the case of the rotation experiment. For the case of light and heavy charge carriers, one would expect the former to dominate the resistivity and the latter to dominate the low field Hall. However, both the resistivity and the AHE are very susceptible to a small perpendicular field.

Finally, we note that for the highest mobility state achieved (blue stars), quantum oscillations are observed in both MR and Hall measurements [Fig.1b, Fig.4b]. These oscillations will be analyzed separately.[18]

Spin-orbit interactions are expected to play a signif-

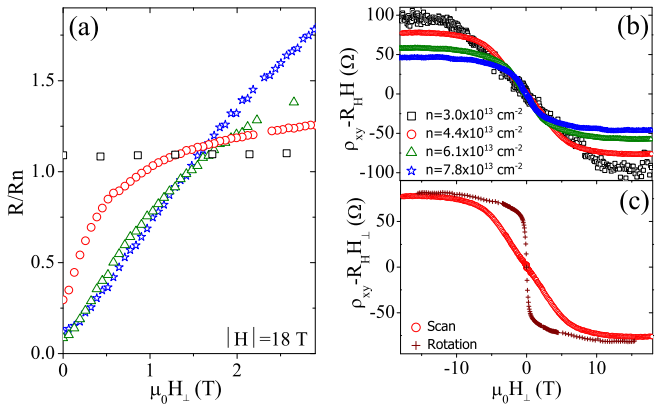

FIG. 4: (Color on-line) a. Normalized resistance as a function of perpendicular magnetic field. Data is taken while rotating the sample in a constant magnetic field of 18 T. b. Hall resistivity after subtraction of a linear fit for high fields (AHE). c. The AHE for $n = 4.4 \times 10^{13} cm^{-2}$ while H is scanned, and while rotating the sample at a constant field.

icant role at the interface due to the inversion symmetry breaking. The SO interaction term is of the form: $\epsilon_{SO} = \mathbf{p} \cdot \sigma \times \nabla V$ where $\mathbf{p}$ is the carrier momentum, σ is the Pauli spinor, and ∇V is the electric field perpendicular to the interface in our system.[19] The strong gate dependence of ϵ_{SO} directly follows from this expression. As pointed out above, the initial local electric field is unknown. When a positive gate voltage was applied for the first time the number of charge carriers decreased, while the resistivity decreased. We believe that this is mainly due to a decrease in the total electric field near the interface, resulting in a decreased SO scattering and an enhanced mobility. This suggests that the initial field (AG state) is a consequence of the electronic reconstruction. In this scenario, adding more $LaAlO_3$ layers increases the as-grown field and hence the SO scattering. This explains the decrease in mobility while increasing the $LaAlO_3$ thickness.[20]

It seems that most scattering processes in the normal-state involve a spin flip, which strongly impede the transport. In a simple metal such processes do not contribute much to the resistivity, yet in our system they become important due to the strong SO coupling. This is clear in the case of in-plane spin flip processes; since SO coupling affects in-plane spin orientations, a spin flip process results in momentum reversal and consequently in a strong contribution to the resistivity. These spins are strongly coupled to the in-plane momenta; therefore it is impossible to align them with $H_{\|}$ unless the energy associated with the field $g\mu_B H_{\|}$ exceeds ϵ_{SO}. For H>H*, the spins gradually align along the field direction and so R_n is reduced. When all spins are aligned, the resistance reaches the saturation value R_{sat}. For the out-of-plane field orientation, suppression of spin scattering is overwhelmed by the large positive MR.

Tuning the gate voltage from 50 to -50 V increases the local electric field, resulting in an increase of ϵ_{SO} and H*. Unlike R_n (the zero field resistance), R_{sat} roughly scales with number of charge carriers deduced from the high field Hall measurements. This suggests that R_{sat} is a result of standard impurity scattering. For Vg=-50 V, ϵ_{SO} is extremely large and an in-plane field of 18 T is not enough to align the spins and suppress the spin-scattering resistivity. Upon applying a small perpendicular field component and due to the large scattering time, orbital motion is immediately turned on along with the SO coupling. This results in a full recovery of the spin-MR.

In summary, we study the phase diagram of the $SrTiO_3/LaAlO_3$ interface in the region where T_c increases, while reducing the carrier concentration by variation of gate voltage. We demonstrate the important effect of spin-orbit (SO) interaction on both superconductivity and on normal-state transport. The SO coupling energy (ϵ_{SO}) is evaluated using two independent transport properties, and is also in agreement with theoretical model given the superconducting parameters: T_c and the upper critical parallel field. ϵ_{SO} follows T_c for the electric field range studied. Our results suggest that $SrTiO_3/LaAlO_3$ interfaces may be useful for future oxide based devices controlling the orbital motion of electrons by acting on their spins. [21]

We are indebted to G. Deutscher, A. Aharony, and Ora Entin-Wohlman for enlightening discussions. This research was partially supported by the Bikura program of the ISF grant No. 1543/08 by the ISF grant No. 1421/08 and by the Wolfson Family Charitable Trust. A portion of this work was performed at the National High Magnetic Field Laboratory, which is supported by NSF Cooperative Agreement No. DMR-0654118, by the State of Florida, and by the DOE.

* yodagan@post.tau.ac.il

[1] S. Okamoto and A. J. Millis, Nature (London) **428**, 630 (2004).
[2] A. Ohtomo and H. Y. Hwang, Nature (London) **427**, 423 (2004).
[3] N. Reyren *et al.*, Science **317**, 1196 (2007).
[4] N. Nakagawa, H. Y. Hwang, and D. A. Muller, Nature Mater. **5**, 204 (2006).
[5] R. Pentcheva and W. E. Pickett, Phys. Rev. Lett. **102**, 107602 (2009).
[6] Z. S. Popović, S. Satpathy, and R. M. Martin, Phys. Rev. Lett. **101**, 256801 (2008).
[7] W. Siemons *et al.*, Phys. Rev. Lett. **98**, 196802 (2007).
[8] P. R. Willmott *et al.*, Phys. Rev. Lett. **99**, 155502 (2007).
[9] M. Basletic *et al.*, Nature Mater. **7**, 621 (2008).
[10] M. Ben Shalom *et at*, Phys. Rev. B **80**, 140403 (2009).
[11] C. Bell *et al*, Phys. Rev. Lett. **103**, 226802 (2009).
[12] A. M. Clogston, Phys. Rev. Lett. **9**, 266 (1962).

[13] J. P. Burger*et al.*, Phys. Rev. **137**, A853 (1965).
[14] N. Reyren *et al.*, Applied Physics Letters **94**, 112506 (2009).
[15] Y. Kozuka *et al.*, Nature **462** (2009).
[16] R. A. Klemm, A. Luther, and M. R. Beasley, Phys. Rev. B **12**, 877 (1975).
[17] S. Seri and L. Klein, Phys. Rev. B **80**, 180410 (2009).
[18] M. Ben Shalom *et al.*, To be published (????).
[19] Y. A. Bychkov and É. I. Rashba, JETP Letters (1984).
[20] C. Bell *et al.*, Applied Physics Letters **94**, 222111 (2009).
[21] S. A. Wolf, Science **294**, 1488 (2001).